

COMPACT GROUPS OF GALAXIES WITH COMPLETE SPECTROSCOPIC REDSHIFTS IN THE LOCAL UNIVERSE

JUBEE SOHN^{1,3}, HO SEONG HWANG², MARGARET J. GELLER³, ANTONALDO DIAFERIO^{4,5}, KENNETH J. RINES⁶,
MYUNG GYOON LEE¹, AND GWANG-HO LEE¹

¹Department of Physics and Astronomy, Seoul National University, Gwanak-gu, Seoul 08826, Korea
jsohn@cfa.harvard.edu

²School of Physics, Korea Institute for Advanced Study, 85 Hoegiro, Dongdaemun-Gu, Seoul 02455, Korea

³Smithsonian Astrophysical Observatory, 60 Garden Street, Cambridge, MA 02138, USA

⁴Dipartimento di Fisica, Università degli Studi di Torino, V. Pietro Giuria 1, I-10125 Torino, Italy

⁵Istituto Nazionale di Fisica Nucleare (INFN), Sezione di Torino, V. Pietro Giuria 1, I-10125 Torino, Italy

⁶Department of Physics and Astronomy, Western Washington University, Bellingham, WA 98225, USA

Received December 1, 2015; accepted December 13, 2015

Abstract: Dynamical analysis of compact groups provides important tests of models of compact group formation and evolution. By compiling 2066 redshifts from FLWO/FAST, from the literature, and from SDSS DR12 in the fields of compact groups in McConnachie et al. (2009), we construct the largest sample of compact groups with complete spectroscopic redshifts in the redshift range $0.01 < z < 0.22$. This large redshift sample shows that the interloper fraction in the McConnachie et al. (2009) compact group candidates is $\sim 42\%$. A secure sample of 332 compact groups includes 192 groups with four or more member galaxies and 140 groups with three members. The fraction of early-type galaxies in these compact groups is 62%, higher than for the original Hickson compact groups. The velocity dispersions of early- and late-type galaxies in compact groups change little with groupcentric radius; the radii sampled are less than $100 h^{-1}$ kpc, smaller than the radii typically sampled by members of massive clusters of galaxies. The physical properties of our sample compact groups include size, number density, velocity dispersion, and local environment; these properties slightly differ from those derived for the original Hickson compact groups and for the DPOSS II compact groups. Differences result from subtle differences in the way the group candidates were originally selected. The abundance of the compact groups changes little with redshift over the range covered by this sample. The approximate constancy of the abundance for this sample is a potential constraint on the evolution of compact groups on a few Gigayear timescale.

Key words: galaxies: evolution — galaxies: groups: general — galaxies: interactions — galaxies

1. INTRODUCTION

Compact groups of galaxies provide a very dense environment for the study of galaxy evolution. These groups contain a few galaxies separated by projected distances of only a few tens of kiloparsec, comparable with the galaxy sizes. Compact groups are thus the densest galaxy systems known. The line-of-sight velocity dispersions of these groups ($\sim 200 \text{ km s}^{-1}$, Hickson et al. 1992) are lower than those of clusters ($500 - 1000 \text{ km s}^{-1}$, Rines & Diaferio 2006; Hwang et al. 2012), but comparable with many loose groups (Einasto et al. 2003). The high density, low velocity dispersion, and short crossing time of compact groups make them a test-bed for the study of galaxy interactions (e.g., Hickson et al. 1992; Mendes de Oliveira & Hickson 1994; Bitsakis et al. 2011; Sohn et al. 2013; Bitsakis et al. 2014; Fedotov et al. 2015).

The physical processes important for the formation and evolution of compact groups remain unclear. The mere survival of these systems for times much longer than a few crossing times has been a long-standing

puzzle. Several numerical simulations showed that galaxies within a compact group should merge and the group should thus disappear (Barnes 1985, 1989; Mamon 1987). In fact, Barnes (1989) proposed that compact group galaxies merge into a single elliptical galaxy on a very short time scale (< 0.02 Hubble time), comparable with the observed crossing time (Hickson et al. 1992; Pompei & Iovino 2012). Other simulations suggested that compact groups can survive much longer than the crossing time (Governato et al. 1991; Athanassoula et al. 1997). Governato et al. (1991) showed that for galaxies with a mass range appropriate to compact groups, some group members may remain in quasi-stable orbits for billions of years. Athanassoula et al. (1997) suggested that compact groups survive because the galaxies are embedded in a common halo. In yet another picture, Diaferio et al. (1994) proposed that compact groups form within a single rich loose group and they can thus acquire new members from the surrounding environment thus lengthening their apparent lifetime. The number density of compact groups as a function of epoch may thus depend not only on the merger rate of galaxies within them but also on the re-

plenishment with new members accreted from the surroundings.

The environments of compact groups are an important clue to understand their formation and evolution. Known compact groups inhabit a range of environments ranging from clusters and rich groups to low density regions. Ramella et al. (1994) found that 76% of a sample of 38 Hickson compact groups are embedded in rich groups. Several studies showed that a significant fraction of compact groups are embedded in clusters, rich groups, less dense poor groups and in the surrounding larger-scale structures (Rood & Struble 1994; Ribeiro et al. 1998; Andernach & Coziol 2005; Mendel et al. 2011; Pompei & Iovino 2012). In some of these studies neither the compact group candidates nor the environments have complete redshift measurements (e.g., see the discussion by Mendel et al. 2011). A fuller understanding of the environmental issues affecting the formation and evolution of compact groups requires complete spectroscopy of compact group candidates within a large volume redshift survey.

The abundance of compact groups as a function of redshift is also a potential constraint on the evolution of these systems. For example, Kroupa (2015) suggested that the abundance of compact groups should decline significantly over a 1 Gyr timescale for halos composed of exotic dark matter particles. The suggestion by Kroupa (2015) tacitly assumes that compact groups do not accrete new members from the environment in contrast with the model proposed by Diaferio et al. (1994). To date there are no direct observational measures of the abundance evolution of compact groups to test these conjectures.

There have been several attempts to construct larger catalogs of compact groups (Rose 1977; Hickson 1982; Prandoni et al. 1994; Iovino et al. 2003; Lee et al. 2004; de Carvalho et al. 2005; McConnachie et al. 2009). Hickson (1982) published a widely used catalog of 100 compact groups. McConnachie et al. (2009) used Hickson's criteria to identify compact groups in the photometric data of the Sloan Digital Sky Survey (SDSS) data release 6 (DR6, Adelman-McCarthy et al. 2008). Currently the sample of McConnachie et al. (2009) is the largest catalog of compact group candidates with 77,088 tentative groups. However, at least 55% of the compact group candidates from the magnitude-limited sample of $14.5 \leq r \leq 18.0$ could be contaminated by interlopers as a result of their selection based on photometric data. This interloper fraction may be greater for their faint sample compact groups with $14.5 \leq r \leq 21.0$.

Redshift surveys of compact group candidates provide a basis for cleaner catalogs better suited to testing models for the formation and evolution of these systems (Hickson et al. 1992; Pompei & Iovino 2012). Hickson et al. (1992) showed that 69 of the 100 compact groups in his original catalog include four or more members with accordant redshifts. Similarly, Pompei & Iovino (2012) observed 138 compact group candidates drawn from the second digital Palomar Observatory Sky Survey (Iovino et al. 2003; de Carvalho et al. 2005); 96

of these contain three or more galaxies with accordant redshifts (DPOSS II compact groups hereafter). The 70% success rate for these two catalogs underscores the importance of spectroscopic observations for constructing a robust sample of compact groups.

We conduct a spectroscopic survey of compact group candidates in the SDSS DR6 to construct an updated sample of compact groups with complete redshifts. By adding 2066 redshifts, we construct the largest catalog of compact groups with complete spectroscopic redshifts. Based on this sample, we examine the physical properties of compact groups including size, velocity dispersion, number density and local environment. We compare these properties with the Hickson and the DPOSS II groups. We show that the physical characteristics of the groups in our catalog are not a strong function of the redshift of the system. We also estimate the abundance of compact groups as a function of redshift for the range $0.01 < z < 0.21$. These estimates are a first step toward using the abundance as a test of models for the evolution of these systems.

Section 2 describes the basic sample used to construct the compact group catalog. Section 3 explains the method of identifying compact group members once the redshifts are measured. We examine the physical properties of the sample compact groups with complete redshifts and compare them with other compact group catalogs in Section 4. We summarize in Section 5. Throughout, we adopt Λ CDM cosmological parameters $H_0 = 100 h \text{ km s}^{-1} \text{ Mpc}^{-1}$, $\Omega_\Lambda = 0.7$, and $\Omega_m = 0.3$.

2. DATA

2.1. Parent Sample

McConnachie et al. (2009) used Hickson's criteria (Hickson 1982) to identify compact group candidates in the photometric sample of SDSS DR6 galaxies. Hickson's criteria can be expressed as follows: $N(\Delta m < 3) \geq 4$, $R_N \geq 3R_G$, and $\mu_{gr} < 26.0 \text{ mag arcsec}^{-2}$. $N(\Delta m < 3)$ means the total number of member candidate galaxies within 3 mag of the brightest galaxy in a system. R_G is the angular size of the smallest circle containing all members, and R_N is the angular size of the largest circle that includes no additional galaxies within 3 mag of the brightest galaxy. μ_{gr} is the mean surface brightness within the circle of radius R_G . McConnachie et al. (2009) constructed two catalogs of compact group candidates with different magnitude limits: catalog A with $14.5 \leq r \leq 18.0$ and catalog B with $14.5 \leq r \leq 21.0$. Catalog A and catalog B list 2297 and 74,791 compact group candidates with 9713 and 313,508 tentative member galaxies, respectively.

Here we use catalog A as a parent sample. Despite the bright magnitude limit for catalog A, only a small fraction of group candidates in the catalog were previously confirmed as genuine compact groups based on spectroscopic redshifts. There are only 70 complete compact groups in the catalog containing four or more members with velocity difference from the mean group velocity less than 1000 km s^{-1} (see Table 1).

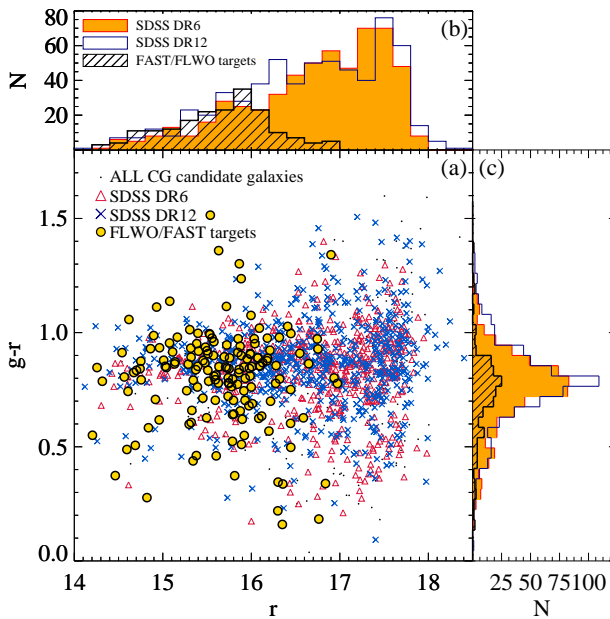


Figure 1. (a) The $g-r$ vs. r color magnitude diagram of FLWO/FAST target galaxies compared with compact group galaxies from SDSS DR6 (triangles, McConnachie et al. 2009) and SDSS DR12 (crosses). Dots indicate compact group candidate galaxies without redshifts. (b)-(c) The r -band magnitude and $g-r$ color distributions for compact group galaxies with SDSS DR6 redshifts (filled histogram), those with SDSS DR12 redshifts (open histogram), and FLWO/FAST target galaxies (hatched histogram).

2.2. Redshift Data

To construct a sample of compact groups with complete redshifts, we conducted a redshift survey of the galaxies in the fields of compact group candidates in catalog A of McConnachie et al. (2009) (see their Table 3). Among the candidate group galaxies, we primarily targeted galaxies in groups that already have two or three members with measured redshifts. We then ranked the targets by their apparent magnitude; the targets have r -band magnitudes in the range $14.2 < r < 17.0$. To avoid other selection effects, we did not use any selection criteria other than apparent magnitude. Figure 1 shows the color-magnitude diagram for the target galaxies. We used the extinction-corrected Petrosian magnitudes from the SDSS DR12. We also plot the compact group galaxies identified with SDSS DR6 and DR12 redshift data. The FAST target galaxies are generally brighter than compact group galaxies with the SDSS redshifts. The color distribution of compact group galaxies peaks at $g-r \sim 0.8$.

We obtained long-slit spectra of 193 galaxies with the FAST spectrograph (Fabricant et al. 1998) installed on the 1.5m Tillinghast telescope at the Fred Lawrence Whipple Observatory (FLWO) from 2013 May to 2014 May. We used a long slit with a 3 arcsec width and a 300 line grating providing spectral resolution of 2.94 \AA and a dispersion of $1.47 \text{ \AA pixel}^{-1}$. The spectra cover the wavelength range $3470\text{--}7420 \text{ \AA}$. The exposure times

range from 900 to 1800 s depending on the brightness of the target galaxy. We reduced the data using IRAF. We measured the redshift of each galaxy with the *russo* (Kurtz & Mink 1998) task. During the pipeline processing, we assigned a quality flag of ‘Q’ for high-quality redshifts, ‘?’ for marginal cases, and ‘X’ for poor fits. We obtained 193 spectra in this study. Among these, five have an ‘X’ flag and three have a ‘?’ flag. We excluded these eight objects from the analysis. The typical velocity measurement error for the FAST spectra of compact group galaxies is 22 km s^{-1} .

We supplemented these data with redshifts from the literature (see Hwang et al. 2010 for details) including the FAST archive and the SDSS DR12 (Alam et al. 2015). There are two redshifts from FAST observations between 2006 and 2008 measured as part of an unpublished study of low-redshift clusters and groups (P.I.: K. Rines). There are 161 and 1718 new redshifts from the literature and SDSS DR12 for galaxies in the fields of compact group candidates in McConnachie et al. (2009). The total number of redshifts we add to the McConnachie et al. (2009) catalog is 2066.

3. A SAMPLE OF COMPACT GROUPS WITH REDSHIFTS

We combine the 2066 additional redshifts with the existing data for galaxies in the fields of compact group candidates in McConnachie et al. (2009). We determine compact group membership based only on galaxies with a spectroscopic redshift.

We first compute the median redshift of compact group member candidates as a tentative group redshift. We then calculate the line-of-sight velocity differences between member candidates and the median redshift, and remove foreground and background galaxies with line-of-sight velocity differences larger than 1500 km s^{-1} . We use the mean velocity of the remaining group galaxies as a group systemic redshift. We finally select member galaxies in each group with concordant redshifts of $|v_{\text{galaxy}} - v_{\text{group}}| \leq 1000 \text{ km s}^{-1}$, following the velocity separation of CG galaxies used in previous studies (Hickson et al. 1992; Mendel et al. 2011; Pompei & Iovino 2012). To check the reliability of the cutoff velocity 1000 km s^{-1} , we test the group selection with the larger cutoff velocities of 1500 km s^{-1} and 2000 km s^{-1} . With the larger cutoff velocities, only a few additional compact group candidates are newly identified as true compact groups. Thus we use cutoff velocity 1000 km s^{-1} for direct comparison with other compact groups based on the same cutoff.

We adopt galaxy morphology information for the compact group galaxies from the Korea Institute for Advanced Study (KIAS) DR7 value-added catalog (VAGC) (Choi et al. 2010). Choi et al. (2010) classified early- and late-type galaxies using the $u-r$ color, the $g-i$ color gradient, and the i band concentration index following the automatic classification scheme suggested by Park & Choi (2005). We visually classify the morphology of galaxies not included in the KIAS DR7 VAGC using the SDSS images.

Table 1
Statistics of Sample Compact Groups

Survey	$N \geq 4$ CGs (members)	$N = 3$ CGs (members)	$N \geq 3$ incomplete CGs (members)
McConnachie et al. (2009)	70 (291)	55 (165)	191 (573)
SDSS DR12	164 (685)	125 (375)	346 (1038)
This study	192 (799)	140 (420)	395 (1185)

There are three types of compact groups in our spectroscopic sample: groups with four or more members ($N \geq 4$ compact groups hereafter), groups with three members ($N = 3$ compact groups hereafter), and incomplete groups with three confirmed members plus one or more tentative member galaxies with unknown redshifts ($N \geq 3$ incomplete compact groups hereafter). We do not use these $N \geq 3$ incomplete groups for further analysis except when computing the group abundance. It is unclear whether these $N \geq 3$ incomplete groups would be confirmed as $N \geq 4$ or $N = 3$ groups; thus we do not include them in the analysis. However, these incomplete groups remain useful for determining the abundance of $N \geq 3$ compact groups. The incomplete compact groups consist of at least three member galaxies and this satisfy our compact group selection criteria. Therefore, we include them only when we compute the group abundance.

Hickson (1982) originally defined compact groups with $N \geq 4$ members rather than with $N \geq 3$ members. Duplancic et al. (2013) compared the properties (i.e., stellar mass, star formation rate and color) of compact triplets with those of larger compact group candidates. They concluded that galaxy triplets do not differ from more populated compact groups, but they do differ from galaxy pairs and clusters. Many previous studies have included $N = 3$ compact groups when all three galaxies have measured redshifts confirming their membership. We thus include the $N = 3$ compact groups.

Table 1 summarizes our compact group selection. In the original catalog of McConnachie et al. (2009), there are 70 $N \geq 4$ and 55 $N = 3$ genuine compact groups with 291 and 165 members, respectively. By adding the SDSS DR12 data, the number of compact groups increases to 164 $N \geq 4$ and 125 $N = 3$ compact groups with 685 and 375 members, respectively. Finally our FLWO/FAST observations contribute an additional 28 $N \geq 4$ and 15 $N = 3$ complete compact groups for a final sample of 192 $N \geq 4$ and 140 $N = 3$ compact groups with 799 and 420 member galaxies, respectively. Among the $N \geq 4$ compact groups, there are 164, 26, 1 and 1 groups with $N = 4, 5, 6$ and 7 members. We also identify 395 $N \geq 3$ incomplete compact groups with a total of 1185 member galaxies. The number of compact groups with complete spectroscopic redshifts in this study is about three times larger than the number in the original McConnachie et al. (2009) catalog.

The new redshift data also identify many chance alignments among the compact group candidates of Mc-

Table 2
Interloper Statistics for Compact Groups

Redshift Survey	N_{tot}^a	N_{int}	f_{int}^a
McConnachie et al. (2009)	958	503	$52.5 \pm 1.6\%$
SDSS DR12	1883	815	$43.3 \pm 1.1\%$
FLWO/FAST	242	83	$34.3 \pm 3.2\%$
Total	2125	898	$42.3 \pm 1.1\%$

^a The number of galaxies in $N \geq 4$ and $N = 3$ compact groups, and chance alignments.

^b Error in the interloper fraction is 1σ standard deviation derived from 1000 bootstrap resamplings.

Connachie et al. (2009). There are 144 and 9 compact group candidates that turn out to be chance alignments of galaxies with discordant redshifts based on the SDSS DR12 and FLWO/FAST data, respectively. This substantial number of chance alignments clearly underscores the importance of spectroscopic redshifts for reducing the contamination of the compact group sample.

The data yield a measure of the interloper fraction for our sample groups. These interlopers are galaxies initially selected as candidate group members, but the redshifts show that they are non-members. We define the interloper fraction as

$$f_{int} = 1 - \frac{N_{members}}{N_{total\ candidates}}, \quad (1)$$

where $N_{members}$ is the number of spectroscopically confirmed members and $N_{total\ candidates}$ is the number of compact group candidate galaxies in the fields of $N \geq 4$ compact groups, $N = 3$ compact groups, and chance alignments. We base the estimate of the interloper fraction on the $N \geq 4$ and $N = 3$ compact groups and chance alignments where most candidate group galaxies in McConnachie et al. (2009) have measured redshifts. We exclude $N \geq 3$ incomplete compact groups and group candidates, because we do not know the exact number of interlopers in these groups. Table 2 lists the numbers of compact group candidate galaxies and the number of interlopers. The interloper fraction we estimate for the original McConnachie et al. (2009) catalog is $52.5 \pm 1.6\%$, consistent with their estimate of 55%. The error in the interloper fraction is the 1σ standard deviation in the interloper fraction obtained with 1000 bootstrap resamplings. The interloper fractions for the

Table 3
A Catalog of Spectroscopically Identified Compact Groups^a

ID ^b	R.A. (J2000)	Decl. (J2000)	n_{mem}	z^c	R_{gr}^c (arcmin)	R_{gr}^c (h^{-1} kpc)	$\log \rho^c$ ($h^3 \text{ Mpc}^{-3}$)	σ^c (km s^{-1})	Nearby cluster ^d
SDSSCGA00027	5.91056	-0.78910	3	0.0633 ± 0.0003	0.325 ± 0.070	16.6 ± 3.6	5.19 ± 4.60	140 ± 20	SDSS-C42022
SDSSCGA00029	204.18318	-3.49931	3	0.0531 ± 0.0000	0.118 ± 0.027	5.1 ± 1.2	6.72 ± 6.17	14 ± 6	
SDSSCGA00035	141.03156	13.21444	4	0.0780 ± 0.0009	0.433 ± 0.076	26.9 ± 4.7	4.69 ± 4.14	500 ± 69	
SDSSCGA00037	10.36639	-9.23039	3	0.0470 ± 0.0001	0.263 ± 0.077	10.2 ± 3.0	5.83 ± 5.28	76 ± 25	
SDSSCGA00042	155.54219	38.52117	4	0.0549 ± 0.0007	0.586 ± 0.131	26.3 ± 5.9	4.72 ± 4.18	470 ± 64	400dJ1020+3831
SDSSCGA00046	127.02769	44.76412	4	0.1465 ± 0.0004	0.267 ± 0.076	28.7 ± 8.2	4.61 ± 4.11	320 ± 73	Abell0667
SDSSCGA00070	157.91676	36.01777	4	0.0861 ± 0.0002	0.401 ± 0.073	27.2 ± 5.0	4.68 ± 4.14	180 ± 29	NSCSJ103122+355649
SDSSCGA00071	31.82000	-1.01116	4	0.1181 ± 0.0010	0.383 ± 0.072	34.3 ± 6.5	4.37 ± 3.81	600 ± 130	
SDSSCGA00090	141.44824	7.72078	4	0.1360 ± 0.0008	0.333 ± 0.075	33.6 ± 7.6	4.40 ± 3.90	540 ± 120	
SDSSCGA00110	147.18958	25.49768	3	0.0455 ± 0.0000	0.344 ± 0.072	12.9 ± 2.7	5.52 ± 4.95	22 ± 7	

^a The complete table is available on-line at <http://astro.snu.ac.kr/~jbsohn/compactgroups/>. A portion is shown here for guidance regarding its form and content.

^b ID from Table 1 in McConnachie et al. (2009).

^c Errors represent the 1- σ standard deviation obtained from by resampling the galaxy sample 1000 times.

^d Known galaxy clusters in NED at $R_{projected} < 1h^{-1}$ Mpc from the group center.

groups we complete with the SDSS DR12 and FLWO/FAST data are slightly smaller than the estimate for the McConnachie et al. (2009) catalog. We add many redshifts of bright galaxies from FLWO/FAST and SDSS DR12 data sets that are more likely to be true members of the groups than the fainter candidates also included in the McConnachie et al. (2009) estimate (see Figure 1).

Table 3 lists 332 compact groups with $N \geq 3$ including ID, R.A., Decl., number of members, group redshift, group size, group number density, velocity dispersion, and neighboring clusters if there are any. The group center is the mean R.A., Decl. and redshift of the member galaxies. We examine whether there are any compact groups close to galaxy clusters using the NASA Extragalactic Database (NED) with the criteria $|v_{group} - v_{cluster}| < 3000 \text{ km s}^{-1}$ and $R_{projected} < 1h^{-1} \text{ Mpc}$, typical virial radius (R_{200}) for galaxy clusters (Rines et al. 2013). Table 4 lists 1473 galaxies in the fields of compact groups in Table 3 including ID, R.A., Decl., morphology, r -band magnitude, $g - r$ color, membership flag, redshifts and its source. We list only the galaxies originally included in the compact group catalog of McConnachie et al. (2009).

In Table 5, we also list 139 galaxies with FLWO/FAST redshifts, not included in the $N \geq 4$ and $N = 3$ compact groups listed in Table 3. Among the 139 galaxies, 49 are in $N \geq 3$ incomplete compact groups and nine galaxies are in chance alignments. The other 81 galaxies are in compact group candidates that could be confirmed as groups if we secure redshifts for the other member galaxies. These groups require further spectroscopy.

4. COMPACT GROUP PROPERTIES

4.1. The Compact Groups

4.1.1. Physical Properties

Figure 2 shows the absolute r -band magnitudes of individual compact group member galaxies as a function of redshift. The sample galaxies are distributed over a redshift range $0.015 < z < 0.212$ and a magnitude range $-22.5 < M_r < -16.0$. The plot shows no significant difference in redshift and magnitude distribution for $N \geq 4$ and $N = 3$ compact group galaxies. For comparison, we plot the absolute r -band magnitudes of the Hickson compact group members. The sample here extends to a higher redshift limit than the Hickson sample.

Figure 3 shows the group velocity dispersion as a function of redshift. The median redshift for our sample is $z = 0.08$. There are more $N = 3$ compact groups than $N \geq 4$ groups at $z > 0.15$, but the most distant compact groups have $N \geq 4$ at $z = 0.211$. There is actually no significant difference in the redshift distribution between the two types of compact groups. The velocity dispersions of $N \geq 4$ and $N = 3$ compact groups appear to increase slightly with redshift, but the errors in the velocity dispersion are too large to identify a clear trend.

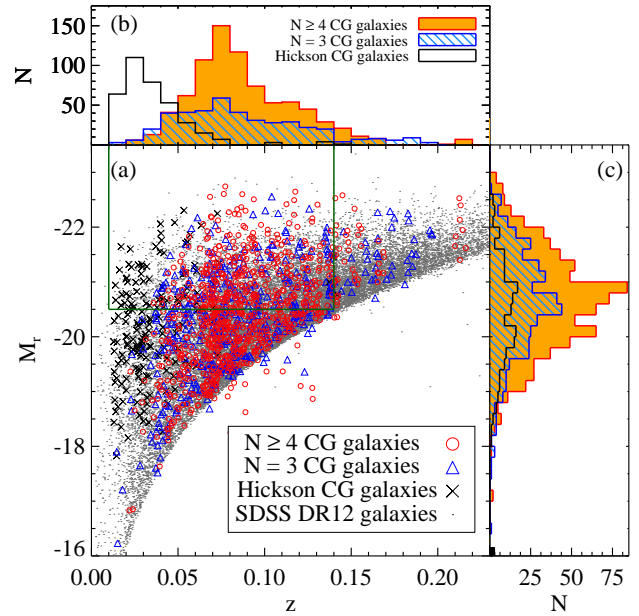


Figure 2. (a) $M_r - z$ diagrams for the galaxies in $N \geq 4$ compact groups (circles) and $N = 3$ complete compact groups (triangles) in our catalog, and for $N \geq 3$ Hickson compact group galaxies (crosses). Small dots indicate SDSS DR12 galaxies (we display only 1% of the data for clarity). The box defines a volume-limited sample of SDSS DR12 galaxies used for computing surrounding galaxy densities (see Section 4). (b) The redshift distributions and (c) the M_r distributions for $N \geq 4$ (filled histogram) and $N = 3$ compact groups (hatched histogram) in our sample and for the Hickson compact group galaxies (open histogram), respectively.

To study the cause of the possible slight increase in the velocity dispersion of compact groups with redshift in Figure 3, we plot the velocity dispersion of compact groups as a function of the total group r -band luminosity (Figure 4). The total luminosity is the sum of r -band luminosities of the members. The velocity dispersion increases with total r -band luminosity; the correlation tests including Pearson's, Spearman's and Kendall's result in correlation coefficients of 0.27-0.38 with the two-sided significance of ~ 0 , indicating a weak, but significant correlation. The distribution for compact groups near galaxy clusters does not differ from the other groups. At higher redshift, compact groups containing only low luminosity member galaxies are undetectable because the limiting absolute magnitude changes with redshift. Thus compact groups at higher redshifts tend to have greater total luminosities and larger velocity dispersion than nearby compact groups. The slight increase in the velocity dispersion of compact groups with redshift in Figure 3 reflects the greater total luminosity of the higher redshift systems. When we examine the velocity dispersions and total luminosities of the DPOSS II compact groups, the compact groups at higher redshift also have larger velocity dispersion and greater luminosity for the same reason.

Table 4
A Catalog of Galaxies in Spectroscopically Confirmed Compact Groups^a

ID ^b	R.A. (J2000)	Decl. (J2000)	Morph. ^c	r	$g - r$	Member ^d	z	z source
SDSSCGA00027.1	5.90833	-0.78417	1	15.42	0.85	1	0.0636 ± 0.00002	SDSS
SDSSCGA00027.2	5.91375	-0.79242	1	16.47	0.90	1	0.0636 ± 0.00002	SDSS
SDSSCGA00027.3	5.90958	-0.79072	1	16.53	0.90	1	0.0627 ± 0.00001	SDSS
SDSSCGA00027.4	5.91083	-0.79033	1	16.94	1.16	0	0.2724 ± 0.00007	SDSS
SDSSCGA00029.1	204.18459	-3.49792	1	14.90	0.83	1	0.0531 ± 0.00015	NED
SDSSCGA00029.2	204.18333	-3.50086	2	15.59	0.79	1	0.0531 ± 0.00008	FLWO
SDSSCGA00029.3	204.18167	-3.49914	1	16.12	1.08	1	0.0530 ± 0.00002	SDSS
SDSSCGA00029.4	204.17500	-3.50419	1	17.58	0.86	0	0.0870 ± 0.00002	SDSS
SDSSCGA00035.1	141.03000	13.21414	1	15.52	0.88	1	0.0789 ± 0.00001	SDSS
SDSSCGA00035.2	141.03749	13.21878	2	14.32	0.90	1	0.0764 ± 0.00012	FLWO

^a The complete table is available on-line at <http://astro.snu.ac.kr/~jbsohn/compactgroups>. A portion is shown here for guidance regarding its form and content.

^b ID from Table 3 in McConnachie et al. (2009).

^c Morphology flag : 1 for early-type galaxies, 2 for late-type galaxies.

^d Membership flag : 1 for members, 0 for non-members, 9 for those without redshifts.

Table 5
A Catalog of FLWO/FAST Target Galaxies, Non-Members of Compact Groups^a

ID ^b	R.A. (J2000)	Decl. (J2000)	r	$g - r$	z
SDSSCGA00012.1	116.18042	16.92258	15.36	0.92	0.0751 ± 0.00009
SDSSCGA00012.2	116.17667	16.92736	15.95	0.85	0.0717 ± 0.00008
SDSSCGA00021.1	178.52542	3.92100	15.32	0.86	0.0747 ± 0.00001
SDSSCGA00023.2	130.04375	8.99811	15.75	0.96	0.0662 ± 0.00015
SDSSCGA00067.1	176.31375	11.49378	15.08	1.13	0.1141 ± 0.00002

^a The complete table is available on-line at <http://astro.snu.ac.kr/~jbsohn/compactgroups>. A portion is shown here for guidance regarding its form and content.

^b ID from Table 3 in McConnachie et al. (2009).

4.1.2. Morphological Content

We next examine the morphological content of compact groups. Both $N \geq 4$ and $N = 3$ compact groups show larger fractions of early-type galaxies than late-type galaxies (Table 6): $65.3 \pm 1.7\%$ and $56.0 \pm 2.3\%$ of $N \geq 4$ and $N = 3$ compact group galaxies are early types, respectively. In total, $62.1 \pm 1.4\%$ of compact group galaxies are early types. This fraction slightly exceeds the fraction of early-type galaxies in the Hickson compact groups ($51 \pm 2\%$, Hickson et al. 1988), but it is smaller than the fraction in the DPOSS II compact groups (81%, Pompei & Iovino 2012). However, the early- and late-type galaxies in the DPOSS II compact groups are classified based on H α equivalent width, different from the morphological approach we take. Therefore, direct comparison is not possible. The fraction of early-type galaxies in our compact groups is similar to the fraction in local galaxy clusters (Park & Hwang 2009).

Figure 5 shows the rest-frame groupcentric velocities of galaxies as a function of projected groupcentric radius (i.e., R-v diagram) for $N \geq 4$ compact groups. We use the group centers in Table 3 (i.e., R.A., Decl. and redshift) to compute the groupcentric radial velocities and the projected groupcentric distances of member galaxies. We then superimpose the groups directly in Figure 5. We distinguish early- and late-type galaxies with different symbols (open circles and

Table 6
Morphological Composition of the Sample Compact Groups

	Early-type galaxies	Late-type galaxies
$N \geq 4$	522 ($65 \pm 1.7\%$)	277 ($35 \pm 1.7\%$)
$N = 3$	235 ($56 \pm 2.3\%$)	185 ($44 \pm 2.3\%$)
Total	757 ($62 \pm 1.4\%$)	462 ($38 \pm 1.4\%$)

triangles). The distribution of projected groupcentric radius for early- and late-type galaxies are similar. The Kolmogorov-Smirnov (K-S) test cannot reject the hypothesis that the radial distributions of the two samples are extracted from the same parent population. The Anderson-Darling (A-D) test gives a result similar to the K-S test. The distributions of the rest-frame groupcentric velocities also show no significant difference. The velocity dispersions of early- and late-type galaxies for $N \geq 4$ compact groups are similar, $259 \pm 9 \text{ km s}^{-1}$ and $266 \pm 14 \text{ km s}^{-1}$, respectively. These results differ from galaxy clusters that typically show higher velocity dispersions for the more centrally concentrated early-type galaxies relative to late-type galaxies (Colless & Dunn 1996; Mahdavi et al. 1999; Hwang & Lee 2008). However, Rines et al. (2013) showed that the velocity distributions of the blue and red galaxies in galaxy clusters are not significantly different, similar to the result we obtain for compact groups.

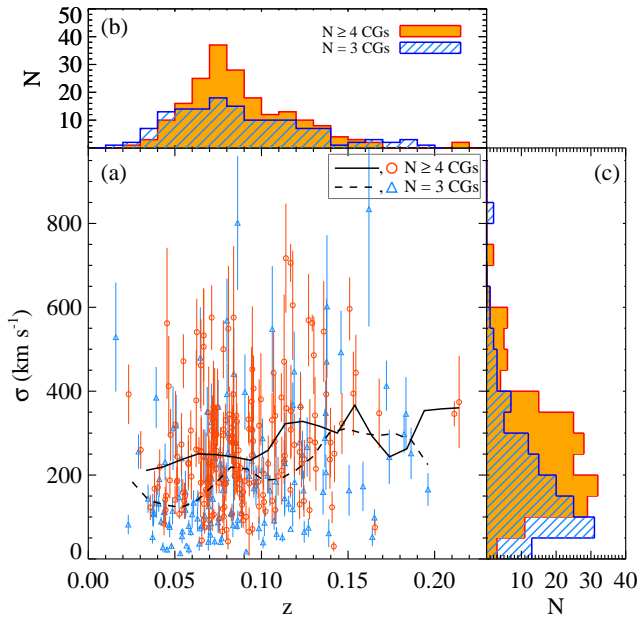


Figure 3. (a) The velocity dispersion (σ) vs. the redshift for $N \geq 4$ compact groups (circles) and for $N = 3$ compact groups (triangles). The solid and dashed lines represent the trend after the Nadaraya-Watson kernel regression smoothing for $N \geq 4$ and $N = 3$ compact groups, respectively. (b) and (c) show the redshift and velocity dispersion distributions for $N \geq 4$ compact groups (filled histogram) and $N = 3$ compact groups (hatched histogram), respectively.

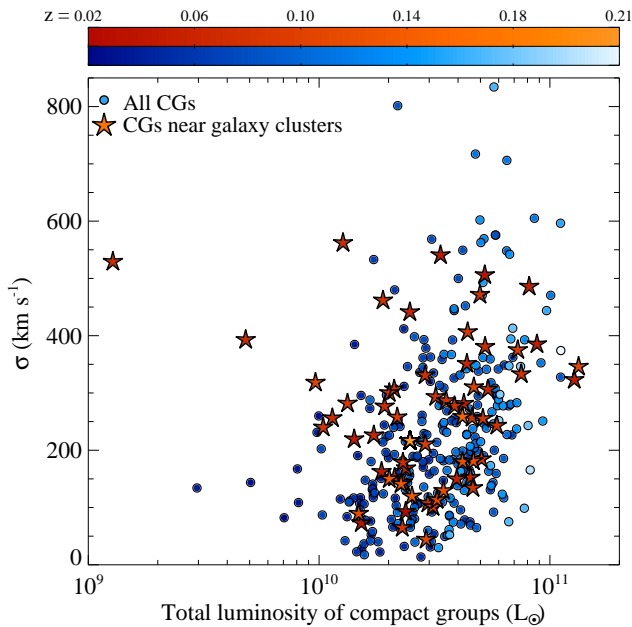


Figure 4. Velocity dispersion vs. total r-band luminosity of compact groups. Circles and starlets show compact groups in normal environments and compact groups within rich clusters, respectively. Lighter colored symbols represent compact groups at higher redshifts.

Figure 6 shows a similar R-v diagram for $N = 3$ compact groups. The projected groupcentric distribu-

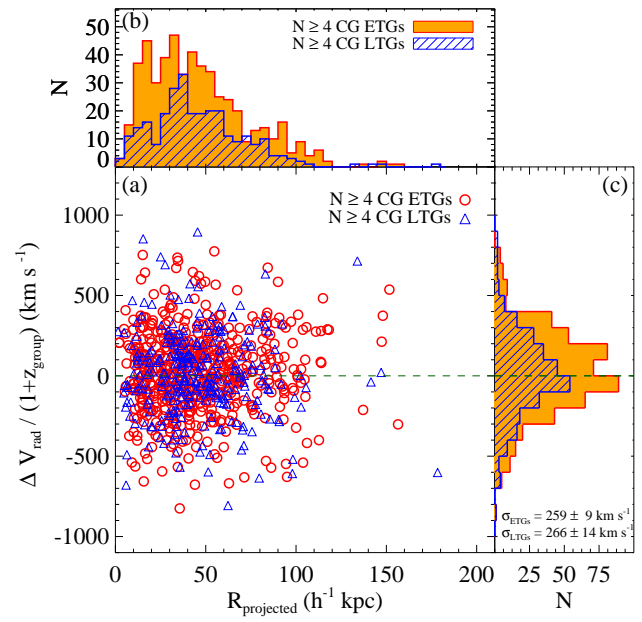


Figure 5. Rest-frame groupcentric radial velocities vs. projected groupcentric distances for $N \geq 4$ compact group galaxies. Circles and triangles represent early- and late-type galaxies, respectively. Their distributions in (b) the projected distances and (c) the radial velocity differences are shown with the filled and hatched histogram, respectively.

tions for early- and late-type galaxies are similar to the $N \geq 4$ compact groups. However, the velocity dispersion of early-type galaxies is significantly larger than for the late-type galaxies ($234 \pm 15 \text{ km s}^{-1}$ vs. $163 \pm 14 \text{ km s}^{-1}$) in contrast with the $N \geq 4$ compact groups.

Figure 7 displays the fraction of early-type galaxies as a function of projected groupcentric distance for $N \geq 4$ and $N = 3$ compact groups. We set the bin size to include a similar number of galaxies in each bin. The fraction of early-type galaxies appears to decrease with groupcentric radius in the range $0 < R_{\text{projected}} < 70 h^{-1} \text{ kpc}$ for both $N \geq 4$ and $N = 3$ compact groups. However, the fraction in the outermost region at $70 < R_{\text{projected}} < 150 h^{-1} \text{ kpc}$ is as high as the fraction in the very inner region. Because we have a similar number of galaxies in each radial bin, this behavior does not simply result from small number statistics.

We also examine the velocity dispersion of early- and late-type galaxies as a function of groupcentric distance. The dispersion profiles do not change much with groupcentric radius except for the innermost region of $N = 3$ compact groups. This result differs from dispersion profiles for galaxy clusters that typically increase with decreasing clustercentric radius (Mahdavi et al. 1999; Biviano & Katgert 2004; Hwang & Lee 2008), but on much larger scale.

Figure 7 shows that we can explore the radial dependence of properties of compact groups (including the early-type fraction and velocity dispersion) in a radial

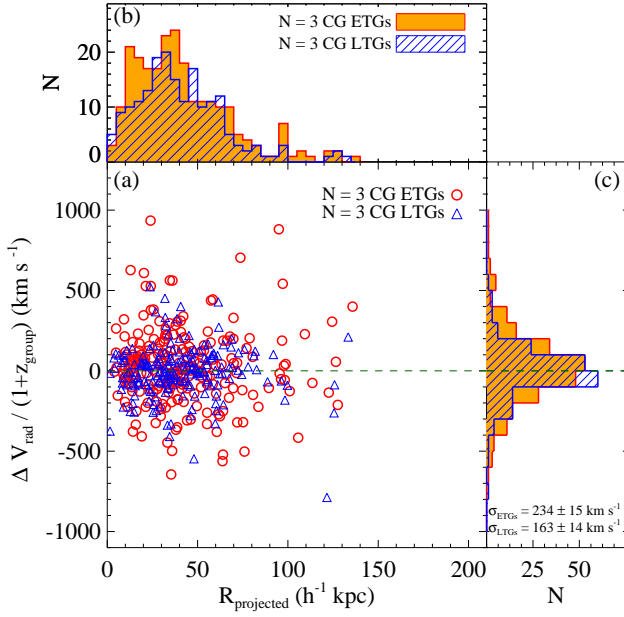


Figure 6. Same as Figure 5, but for $N = 3$ compact groups.

range $0 < R_{\text{projected}} < 150 h^{-1} \text{ kpc}$. This small range is interesting because it is hard to sample in any other systems. The scale is, for example, comparable to or smaller than the typical size of the brightest cluster galaxies ($\sim 100 \text{ kpc}$, Newman et al. 2013; López-Cruz et al. 2014). The morphological properties of galaxies in these small dense regions may ultimately provide interesting tests of processes involved in galaxy evolution.

4.1.3. The Abundance of Compact Groups

Figure 8 plots the abundance of compact groups as a function of redshift. To compute the abundance, we first count all of the compact groups in McConnachie et al. (2009) including the $N \geq 4$ compact groups, $N = 3$ compact groups, and $N \geq 3$ incomplete compact groups in the volume of SDSS DR7 main galaxy survey. Although the $N \geq 3$ incomplete compact groups are not included in our compact group catalog, they are useful for determining the abundance of $N \geq 3$ compact groups. Because we use a magnitude-limited sample of galaxies to identify compact groups, the variation in the absolute magnitude limit as a function of redshift affects the observed abundance of compact groups.

To correct for this effect, we follow the method of Barton et al. (1996), who computed the abundance of compact groups identified by applying a friends-of-friends method to the magnitude-limited sample of CfA2+SSRS2 redshift survey data (Geller & Huchra 1989; Giovanelli & Haynes 1985; da Costa et al. 1994). Barton et al. (1996) assumed that the galaxies in their sample compact groups are randomly drawn from a magnitude distribution $\bar{\Phi}(M)$. They then calculated P_i , the probability for detecting i th brightest member of a compact group in the absolute magnitude range $[M, M + dM]$. The P_i is proportional to $P_{(i-1) < M}(M) \bar{\Phi}(M) dM$, where $P_{(i-1) < M}(M)$ is the

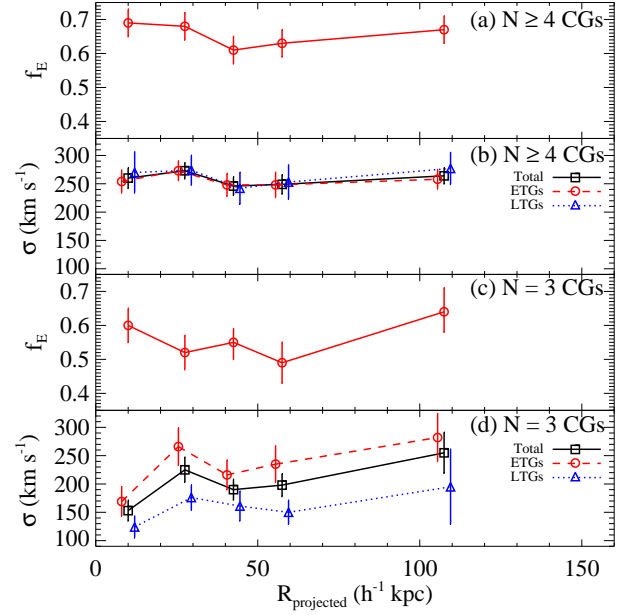


Figure 7. (a) Fraction of early-type galaxies vs. projected distances from the group center for $N \geq 4$ compact groups. (b) The velocity dispersion of all $N \geq 4$ member galaxies (square-solid lines), early- (circle-dashed lines), and late-type galaxies (triangle-dotted lines). Each point is arbitrarily shifted along the x-axis for clarity. (c) and (d) panels are the same as (a) and (b), but for $N = 3$ compact groups.

probability that $i - 1$ group members are brighter than M . They derived the $P_{(i-1) < M}(M)$ from the Poisson distribution:

$$P_{(i-1) < M} = \frac{e^{-\lambda_M} \lambda_M^{(i-1)}}{(i-1)!}, \quad (2)$$

where λ_M is the average number of galaxies in a group brighter than M :

$$\lambda_M = \kappa \int_{-\infty}^M \bar{\Phi}(M') dM'. \quad (3)$$

Here, κ is a normalization parameter, and is a function of redshift. Finally, they expressed the probability of detecting $\geq i$ group member galaxies:

$$\begin{aligned} P_{\text{detection}}(z) &= \frac{1}{A} \int_{-\infty}^{M_{\text{lim}}(z)} P_i(M) dM \\ &= \frac{1}{A} \int_{-\infty}^{M_{\text{lim}}(z)} \frac{e^{-\lambda_M} \lambda_M^{(i-1)}}{(i-1)!} \bar{\Phi}(M) dM, \end{aligned} \quad (4)$$

where $M_{\text{lim}}(z)$ is the limiting absolute magnitudes at the redshift, and A is the normalization factor which makes $P_{\text{detection}}(z = 0) = 1$.

Following the method in Barton et al. (1996), we construct the selection function for our sample compact groups. We use the luminosity function determined from nearby galaxies in the SDSS data: a Schechter function with $\alpha = -0.918 \pm 0.027$ and $M_{\text{star}} = -20.31 \pm$

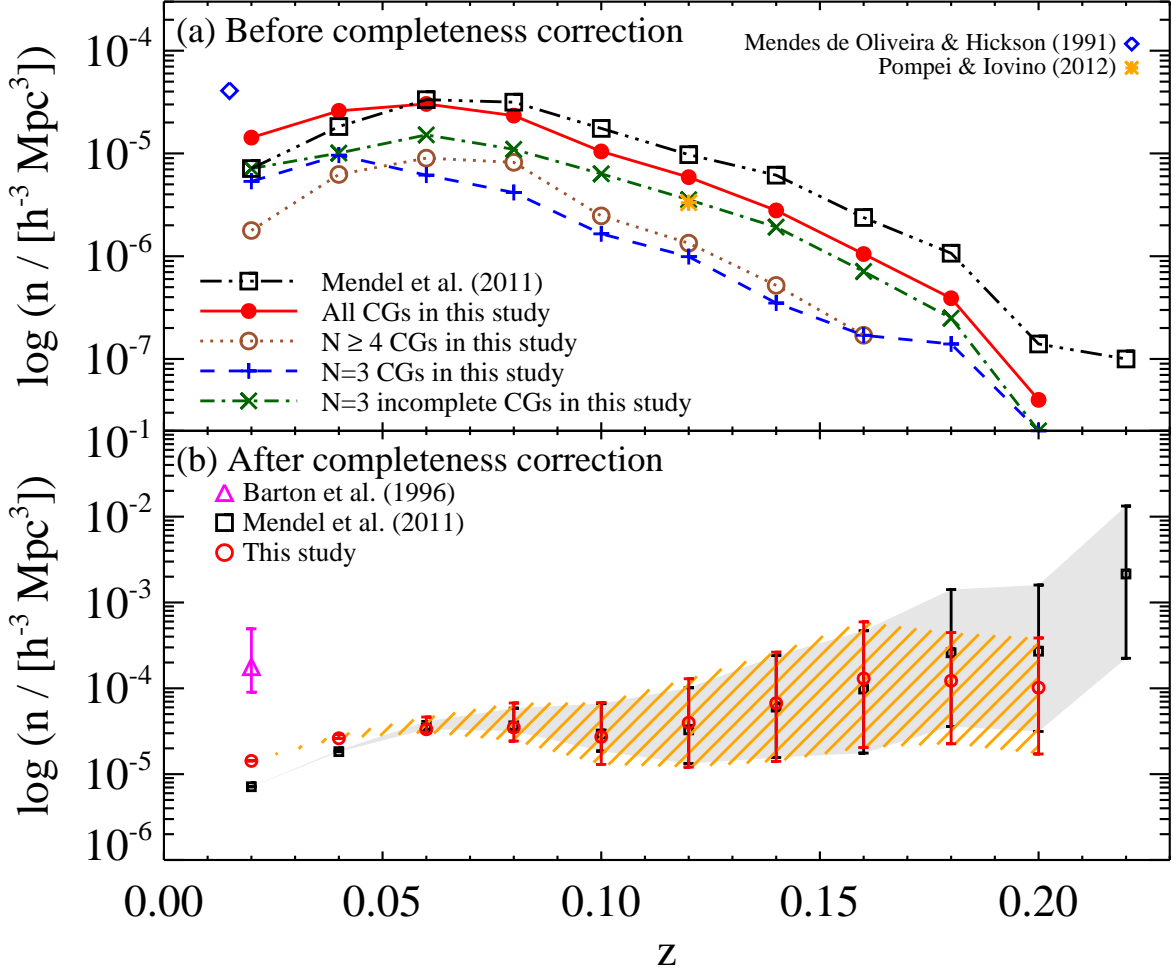


Figure 8. The abundance of compact groups as a function of redshift (a) before the redshift effect correction and (b) after the correction. The abundances of other compact groups are shown for comparison; the Hickson compact groups (diamond, Mendes de Oliveira & Hickson 1991), the CfA2 compact groups (triangle, Barton et al. 1996), the SDSS DR7 compact groups identified by photometric redshifts (square, Mendel et al. 2011), and the DPOSS II compact groups (asterisk, Pompei & Iovino 2012). The symbols are shown at the mean redshift for each group survey.

0.04 from a volume-limited sample of galaxies with $0.025 < z < 0.044$ and $M_r < -18.0$ (Choi et al. 2007). We use fixed κ , the median of the measured κ for each compact group. To estimate the uncertainty in the selection function, we determine the upper and lower limits for the selection function using the 1st and 3rd quartiles of κ . Then, we derive the detection probability for compact groups P_i using Equation (3).

Finally, we calculate the volume number density of compact groups (n_{cg})

$$n_{cg} = \frac{N}{\frac{\Omega_{survey}}{\Omega_{all\ sky}} \int_{z_i}^{z_f} \frac{4}{3} \pi D_c(z)^3 P_{detection}(z) dz}, \quad (5)$$

where N is the total number of $N \geq 4$ and $N = 3$ compact groups and $N \geq 3$ incomplete groups in the redshift range. In Equation (5), Ω_{survey} and $\Omega_{all\ sky}$ are, respectively, the solid angles of the SDSS DR7 (8032 deg²) and the full sky, and D_c is the comoving distance. We also calculate the 1st and 3rd quartile of the

abundance of compact groups using the corresponding κ . We take these values as upper and lower limits.

Before we apply the completeness correction, we estimate the mean abundance for compact groups at the $z = 0.1$ to compare with result from the literature (Mendel et al. 2011; Pompei & Iovino 2012). We use the Equation (1) of Lee et al. (2004) to estimate the mean abundance. The mean abundance for our sample compact groups is $1.76 \times 10^{-5} h^3 \text{ Mpc}^{-3}$, similar to that for the sample of Mendel et al. (2011) ($\sim 2.59 \times 10^{-5} h^3 \text{ Mpc}^{-3}$), but larger than for the DPOSS II compact groups ($\sim 3.32 \times 10^{-6} h^3 \text{ Mpc}^{-3}$, Pompei & Iovino 2012). We note that the DPOSS II compact group abundance accounts only for ‘isolated’ groups. The estimate of Mendel et al. (2011) is exceeding our result even though they used only $N \geq 4$ compact groups. Because Mendel et al. (2011) identified their sample groups using photometric redshifts and did not apply a completeness correction, they may overestimate the compact group abundance. In addi-

tion, several studies have estimated the mean group abundance (Mendes de Oliveira & Hickson 1991; Iovino et al. 2003; Lee et al. 2004; de Carvalho et al. 2005; Díaz-Giménez et al. 2012), but it is difficult to compare these abundances with our result because of differences in the selection criteria and the lack of a completeness correction.

The bottom panel shows that the abundance of our sample compact groups as a function of redshift after the completeness correction. We also plot the abundance for the compact group sample of Mendel et al. (2011) after a similar completeness correction. We note that the sample from Mendel et al. (2011) is derived from photometric redshifts, and only contains $N \geq 4$ compact groups.

The abundances of compact groups in this study and in Mendel et al. (2011) at low redshift (i.e., $z \sim 0.02$) appear smaller than the abundance of the CfA2 compact groups (Barton et al. 1996). This difference could result from the Hickson’s isolation criterion. The isolation criterion requires that there be no other galaxies within three magnitudes of the brightest group galaxy within the isolation annulus ($R_G < R_{GCD} < 3R_G$, where R_{GCD} is groupcentric distance). This criterion was introduced to avoid very dense regions like cluster cores, but it tends to reject some nearby groups. In general, the spatial extent of nearby groups are larger than for distant groups. Thus, the isolation annulus for nearby groups is larger than that for high-redshift groups and some nearby compact groups with large spatial extent may not be selected as compact groups because there are many interlopers within the isolation annulus. The compact groups in this study and in Mendel et al. (2011) are identified with Hickson’s criterion, but the compact groups in Barton et al. (1996) are selected with a friends-of-friends algorithm. We plan to examine this issue further using a method similar to Barton et al. (1996), but with a large spectroscopic sample of galaxies.

The abundance of our sample compact groups changes little as a function of redshift. The sample of Mendel et al. (2011) also changes little with redshift. These results are consistent with Barton et al. (1996), who showed that the abundance of compact groups does not change in the redshift range $0.00 < z < 0.03$ when the compact groups are identified directly from a spectroscopic sample of galaxies using the friends-of-friends algorithm. Kroupa (2015) suggested that there would be more compact groups 1 Gyr ago (e.g., $z \sim 0.1$) than in the current universe if compact groups collapse into a single elliptical galaxies on a short timescale. Our results suggest that the abundance of compact groups does not change significantly with redshift. Thus compact groups either survive longer than 1 Gyr or they are replenished with galaxies from the surrounding region.

4.2. Comparison with Other Compact Group Samples

To compare the physical properties of the compact groups in this study with those in previous studies, we use samples of compact groups based on similar selec-

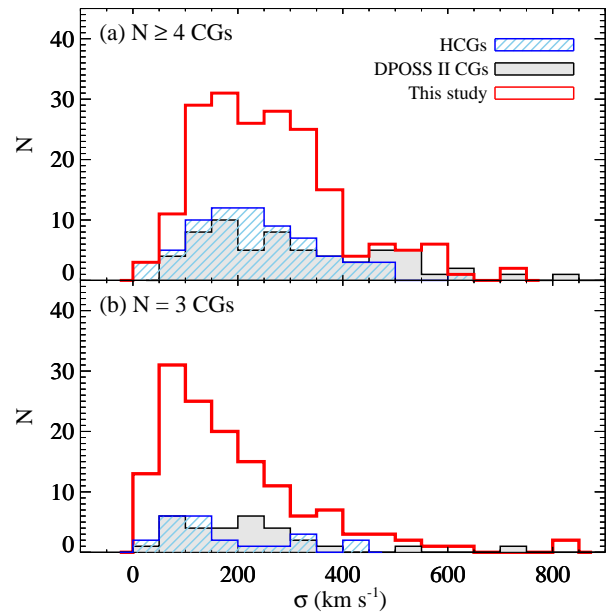


Figure 9. Distribution of group velocity dispersion (σ) for $N \geq 4$ compact groups and $N = 3$ compact groups in our samples (open histogram) compared with the Hickson compact groups (hatched histogram) and the DPOSS II compact groups (filled histogram).

tion criteria and on redshift survey data: Hickson compact groups (Hickson et al. 1992) and DPOSS II compact groups (Pompei & Iovino 2012). The Hickson compact groups are in the redshift range $0.003 < z < 0.333$ and they include member galaxies with $r < 19.5$. The DPOSS II compact groups span a redshift range $0.044 < z < 0.233$ and the magnitudes of the member galaxies are $r < 19.0$.

Both samples are based on Hickson’s selection criteria, but the selection criteria for the DPOSS II compact groups differ slightly from Hickson’s. Iovino et al. (2003) and de Carvalho et al. (2005) used: $N(\Delta m < 2) \geq 4$, $R_N \geq 3R_G$, and $\mu_G \leq 24.0$ mag arcsec $^{-2}$. These criteria differ from Hickson’s in several ways. First, Hickson used $N(\Delta m < 3)$ rather than $N(\Delta m < 2)$, where $N(\Delta m < 2)$ refers to the total number of galaxies within 2 mag of the brightest member galaxy. Second, R_N in Hickson’s criteria is the angular size of the smallest circle encompassing no additional galaxies within 3 mag of the brightest group member, while R_N for the DPOSS II compact groups is the angular size of the largest circle that includes no additional galaxies within 0.5 mag of the faintest group member. The definitions of R_G are the same. Third, the mean surface brightness limit for Hickson’s criteria is 26.0 mag arcsec $^{-2}$ rather than 24.0 mag arcsec $^{-2}$. These differences between the DPOSS II and the Hickson account for some of the differences in the physical properties of compact groups in the two samples.

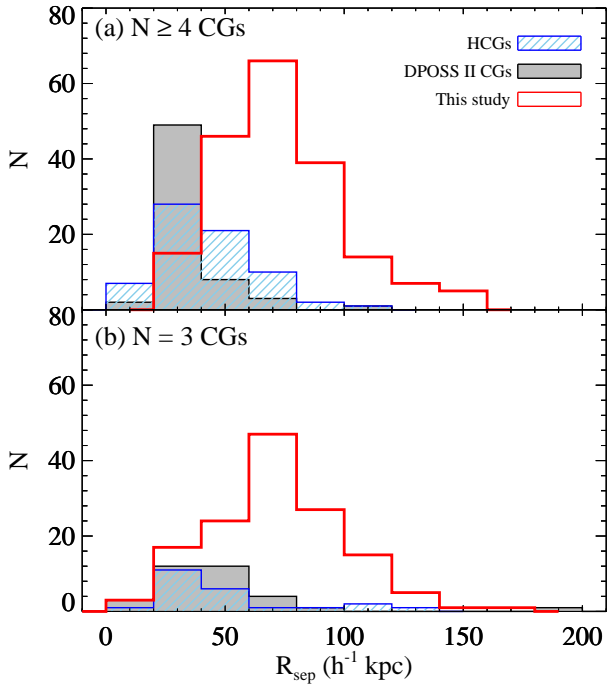


Figure 10. Distribution of the median projected separation (R_{sep}) of member galaxies for (a) $N \geq 4$ compact groups and (b) $N = 3$ compact groups. The histograms are as in Figure 9.

4.2.1. Physical Properties

We estimate the velocity dispersion for our sample compact groups following Danese et al. (1980); the dispersions range from 13 km s^{-1} to 834 km s^{-1} with a typical error of 44 km s^{-1} (Figure 9). The median velocity dispersion of all, $N \geq 4$, and $N = 3$ compact groups are, respectively, $207 \pm 12 \text{ km s}^{-1}$, $244 \pm 11 \text{ km s}^{-1}$ and $160 \pm 14 \text{ km s}^{-1}$. Here, the errors of median values indicate 1σ standard deviation from 1000 times bootstrap resamplings. These results are similar to the Hickson compact groups (median(σ) = $204 \pm 13 \text{ km s}^{-1}$), but smaller than for the DPOSS II compact groups (median(σ) = $251 \pm 22 \text{ km s}^{-1}$). When we compare the velocity dispersions of $N \geq 4$ and $N = 3$ compact groups separately, the velocity dispersions of the DPOSS II compact groups still exceed those for other two samples.

Figure 10 shows the distribution of the median projected separation of member galaxies in our sample compared with the Hickson and the DPOSS II groups. Our sample compact groups have a median projected separation (R_{sep}) ranging from $11 h^{-1} \text{ kpc}$ to $167 h^{-1} \text{ kpc}$; this range is similar to that of other compact groups: $2 h^{-1} \text{ kpc}$ to $135 h^{-1} \text{ kpc}$ for the Hickson compact groups and $12 h^{-1} \text{ kpc}$ to $188 h^{-1} \text{ kpc}$ for the DPOSS II compact groups. However, the median projected separation of our sample compact groups is larger (median $R_{\text{sep}} \sim 72 h^{-1} \text{ kpc}$) than that for the Hickson compact groups (median $R_{\text{sep}} \sim 39 h^{-1} \text{ kpc}$) and the DPOSS II compact groups (median $R_{\text{sep}} \sim 34 h^{-1}$

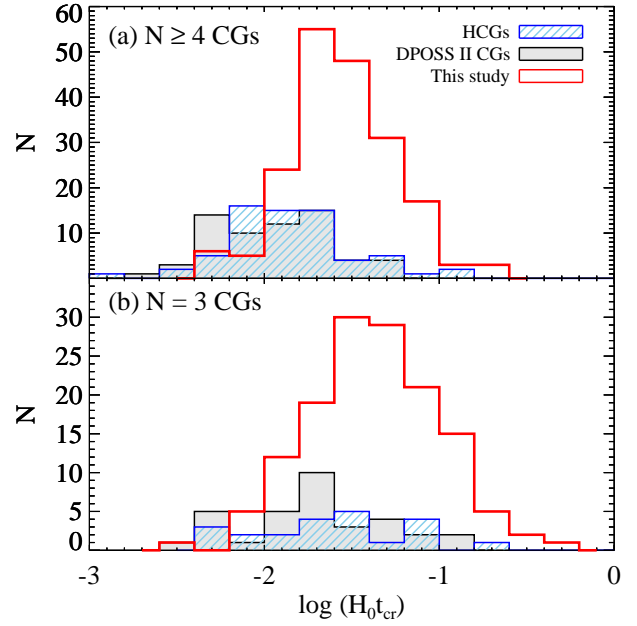


Figure 11. Distribution of the crossing time for (a) $N \geq 4$ compact groups and (b) $N = 3$ compact groups. The histograms are as in Figure 9.

kpc). When we compare $N \geq 4$ and $N = 3$ compact groups separately, these differences remain. The group radius of our sample compact groups (median $R_G \sim 57.8 \pm 1.5 h^{-1} \text{ kpc}$) is also larger than that of the Hickson compact groups (median $R_G \sim 38.6 \pm 7.1 h^{-1} \text{ kpc}$), but similar to that of the our parent sample (median $R_G \sim 62 h^{-1} \text{ kpc}$ McConnachie et al. 2009).

We also derive the crossing times of the compact groups (Figure 11). The crossing time is

$$t_{cr} = \frac{4R_{\text{sep}}}{\pi\sigma_{3D}}, \quad (6)$$

where R_{sep} is the median galaxy-galaxy separation and σ_{3D} is the three-dimensional velocity dispersion (see Equations (1) and (2) in Hickson et al. 1992). The dimensionless crossing time ($H_0 t_{cr}$) for our sample compact groups ranges from 0.004 to 0.469, similar to the distributions of the Hickson and the DPOSS II compact groups. The median crossing time (0.033 ± 0.003) for our sample compact groups is larger than for the Hickson (0.016 ± 0.131) and for the DPOSS II (0.015 ± 0.002) compact groups. The larger crossing time of our sample compact groups results from the larger inter-galaxy separations compared with other compact groups.

We compute the group density as in Barton et al. (1996)

$$\rho = \frac{3N}{4\pi R_G^3} \quad (7)$$

where N is the number of member galaxies, and R_G is the group radius in $h^{-1} \text{ Mpc}$. Figure 12 displays the distribution of densities for our sample and for Hickson's sample. The number densities in our sample are lower than for the Hickson compact groups because the

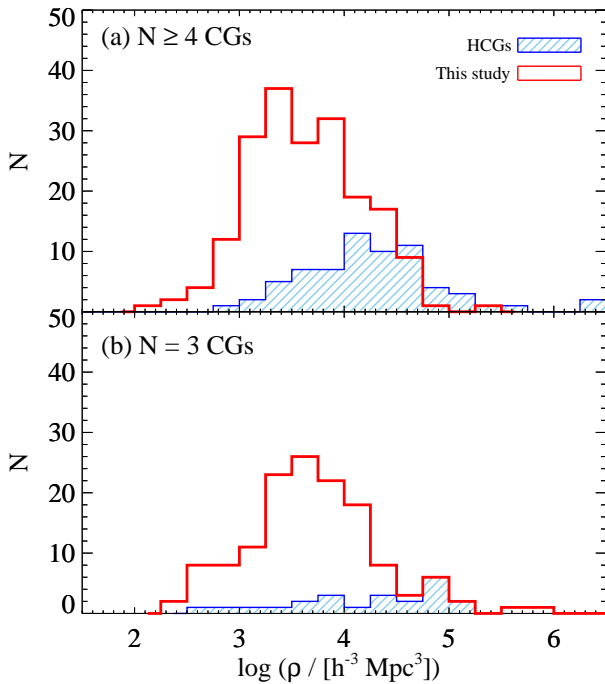


Figure 12. Distribution of galaxy number density within groups for (a) $N \geq 4$ compact groups and (b) $N = 3$ compact groups. The histograms are as in Figure 9, but the density distribution of the DPOSS II compact group is not shown here.

sizes of our compact groups are, on average, larger than for the Hickson compact groups. The median number density for our sample is $\log(\rho/[h^{-3} \text{ Mpc}^3]) = 3.65$, substantially exceeding the number density for subclusters and subgroups in the A2199 superclusters (the median number density at $R < 0.5 R_{200}$ is $\log(\rho/[h^{-3} \text{ Mpc}^3]) = 1.97$, Lee et al. 2015). Compact groups are indeed much denser environments than galaxy clusters. Table 7 summarizes the physical properties of the compact groups in this study compared with the Hickson and the DPOSS II samples.

4.2.2. Local Environments of Compact Groups

Figure 13 displays an example of the spatial distribution of compact groups relative to the surrounding large-scale structure for a slice of $9^h < \alpha_{2000} < 16^h$ and $12.5^\circ < \delta_{2000} < 13.5^\circ$. We choose this slice to show various environments of compact groups even though there are only four compact groups in this thin slice. To show homogeneous structures of galaxies regardless of redshift, we plot galaxies in a volume-limited sample with $M_r < -20.5$ and $0.00 < z < 0.14$ (see the large box in Figure 2). As expected based on previous studies of smaller samples (Rood & Struble 1994; Ramella et al. 1994; Ribeiro et al. 1998; Andernach & Coziol 2005; Pompei & Iovino 2012), the environments of compact groups are diverse (Figure 14).

In Table 3, we examine the number of compact groups located near galaxy clusters. Using NED and requiring $|v_{\text{group}} - v_{\text{cluster}}| < 3000 \text{ km s}^{-1}$ and

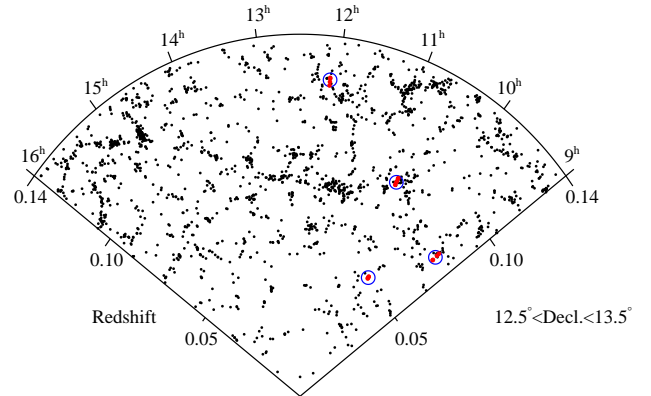


Figure 13. Example cone diagram for a slice of $9^h < \alpha_{2000} < 16^h$, $12.5^\circ < \delta_{2000} < 13.5^\circ$, and $0.00 < z < 0.14$. Large open and small filled circles indicate compact groups and their member galaxies, respectively. Small dots denote SDSS galaxies in a volume limited sample with $M_r < -20.5$ and $0.01 < z < 0.14$. The Σ_5 for the compact groups from the right are $\Sigma_5 = 16.08, 0.07, 0.67$ and 0.19 .

$R_{\text{projected}} < 1 h^{-1} \text{ Mpc}$, only 69 (21%) of our sample compact groups are near known massive clusters. With more relaxed criteria, $|v_{\text{group}} - v_{\text{cluster}}| < 6000 \text{ km s}^{-1}$ and $R_{\text{projected}} < 1 h^{-1} \text{ Mpc}$ (Mendel et al. 2011), the number of compact groups near known massive clusters changes little to 80 (i.e., 24%). These fractions are smaller than those in previous studies; e.g., 35% in Pompei & Iovino (2012) and 50% in Mendel et al. (2011) based on similar criteria. Mendel et al. (2011) used compact groups identified with photometric redshifts and $N > 4$ galaxy groups from the SDSS DR7 (Tago et al. 2010) to study the local environments of compact groups. In contrast, we use only compact groups with complete spectroscopic redshifts and known massive galaxy clusters listed in NED; thus our criteria are stricter than in other studies. The more restrictive criteria result in the lower fraction of compact groups within known massive clusters.

We also investigate the local environments of our sample compact groups using the parameter, Σ_5 , and compare them with the environments of the Hickson and the DPOSS II compact groups. Σ_5 is the surface number density defined as $\Sigma_5 = 5(\pi D_{p,5}^2)^{-1}$, where $D_{p,5}$ is the projected distance between the center of the compact group and the fifth nearest neighbor galaxy. We use galaxies in the volume-limited sample to compute the nearest neighbor densities and to make a fair comparison regardless of redshift. We use neighbor galaxies with relative velocities $\Delta v < 1500 \text{ km s}^{-1}$, and compute Σ_5 relative to the center of each compact group. We obtain Σ_5 for 309 groups within the volume-limited sample.

Figure 14 shows the Σ_5 distribution for our sample compact groups along with the Hickson and the DPOSS II compact groups for the redshift range $0.01 < z < 0.14$. Some groups in our study are in denser environment than the Hickson compact groups. Indeed, the A-D test rejects the hypothesis that the distributions

Table 7
Basic Properties of Compact Groups

Samples	Types	N_{gr}	N_{gal}	R_{group}^a (h^{-1} kpc)	$\log \rho^a$ ($h^3 \text{Mpc}^{-3}$)	R_{sep}^a (h^{-1} kpc)	σ^a (km s^{-1})	$H_0 t_{cr}^a$
This study ($0.016 < z < 0.211$)	Total	332	1129	57.8 ± 1.5	3.65 ± 0.03	71.7 ± 1.4	$207. \pm 12.$	0.033 ± 0.003
	$N \geq 4$	192	799	62.4 ± 2.0	3.64 ± 0.04	70.5 ± 1.9	$244. \pm 11.$	0.028 ± 0.002
	$N = 3$	140	420	54.1 ± 2.4	3.66 ± 0.05	73.4 ± 2.4	$160. \pm 14.$	0.042 ± 0.005
Hickson Compact Groups ($0.003 < z < 0.333$)	Total	92	382	38.6 ± 7.1	4.27 ± 0.09	39.8 ± 2.4	$204. \pm 13.$	0.016 ± 0.131
	$N \geq 4$	69	313	40.1 ± 9.1	4.21 ± 0.11	39.9 ± 2.6	$209. \pm 15.$	0.012 ± 0.138
	$N = 3$	23	69	30.2 ± 5.6	4.4 ± 0.17	38.0 ± 6.7	$123. \pm 26.$	0.025 ± 0.325
DPOSS II Compact Groups ($0.044 < z < 0.233$)	Total	96	370	--	--	34.2 ± 2.3	$251. \pm 22.$	0.015 ± 0.002
	$N \geq 4$	63	271	--	--	31.4 ± 1.9	$278. \pm 32.$	0.012 ± 0.002
	$N = 3$	33	99	--	--	40.4 ± 5.4	$215. \pm 30.$	0.020 ± 0.006

^a The median of each parameter are listed. The errors are 1σ standard deviations derived from 1000 bootstrapping resamplings.

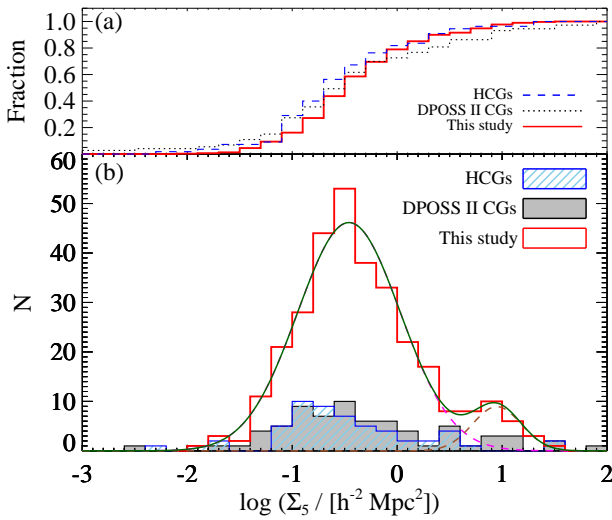


Figure 14. (a) Cumulative distribution of the surrounding surface number density (Σ_5) and (b) the distribution of Σ_5 for our sample compact groups (solid line, open histogram) the Hickson compact groups (dashed line, hatched histogram), the DPOSS II compact groups (dotted line, filled histogram).

of all three samples are extracted from the same parent population with a low p-value (< 0.1).

Figure 14 suggests that the Σ_5 distribution of compact groups can be divided into two as many previous studies suggested: ‘isolated’ and ‘embedded’ compact groups. To examine the multiplicity of the Σ_5 distribution, we use a statistical test, the Gaussian mixture model (GMM, Muratov & Gnedin 2010). The GMM evaluates whether the data are more consistent with a multimodal Gaussian distribution rather than a unimodal Gaussian distribution. If the data consist of multiple populations, the GMM returns 1) a low parametric bootstrap method probability, 2) a large separation ($D > 2$) between multiple Gaussian peaks, 3) a negative *kurtosis* of the input distribution, and 4) a larger enhancement of the likelihood for the multimodal case than for the unimodal case ($-2 \ln(L_{unimodal}/L_{multimodal})$).

We assume that there are two populations of com-

compact groups with high and low Σ_5 , and apply the GMM. The GMM test indicates that the Σ_5 distribution may have a bimodal distribution with low probability $p = 6.97 \times 10^{-6}$, *kurtosis* $k = 0.186 \pm 0.824$, large separation between peaks $D = 3.68 \pm 0.53$, and large enhancement of the likelihood $-2 \ln(L_{unimodal}/L_{multimodal}) = 29.3$. This means that the Σ_5 distribution is consistent with bimodal distribution. The two populations of compact groups are divided at $\log(\Sigma_5) = 0.62$, and 91% (281 out of 309) of compact groups belong to a population with low Σ_5 . If we accept this bimodal distribution of Σ_5 and Σ_5 traces the local environments of compact groups, only $\sim 9\%$ of compact groups are in dense environments. This fraction is much lower than in previous studies (33 – 50%), but our division is based on a statistical test that is very strict compared with other studies based on different local environment indicators (e.g., distance to nearby galaxy groups). Hereafter, we refer the compact groups in dense environments as ‘embedded’ groups, and the others as ‘isolated’ groups.

Figure 15 plots the physical properties of the isolated and the embedded compact groups including group radius, velocity dispersion, crossing time, and number density. The median size of embedded groups ($43.3 \pm 4.0 h^{-1}$ kpc) is smaller than for isolated groups ($57.8 \pm 1.4 h^{-1}$ kpc). The discrepancy also exists even when we compare the $N \geq 4$ and $N = 3$ compact groups separately. This result is consistent with previous studies based on different compact group samples (Mendel et al. 2011; Díaz-Giménez & Zandivarez 2015). The smaller sizes of embedded groups result in lower number densities than for isolated groups (Figure 15 (d)). The size and density distributions of the two groups are drawn from significantly different distributions as the A-D test suggests with low p-value < 0.01 . The median velocity dispersion of embedded groups ($316 \pm 25 \text{ km s}^{-1}$) is significantly larger than that of isolated groups ($219 \pm 8 \text{ km s}^{-1}$). The distributions of velocity dispersions of the two groups are also different. This is also consistent with the results in Pompei & Iovino (2012) for the DPOSS II compact groups. Therefore, the median crossing time of embedded compact groups is shorter than the isolated compact groups. The distributions of crossing time for

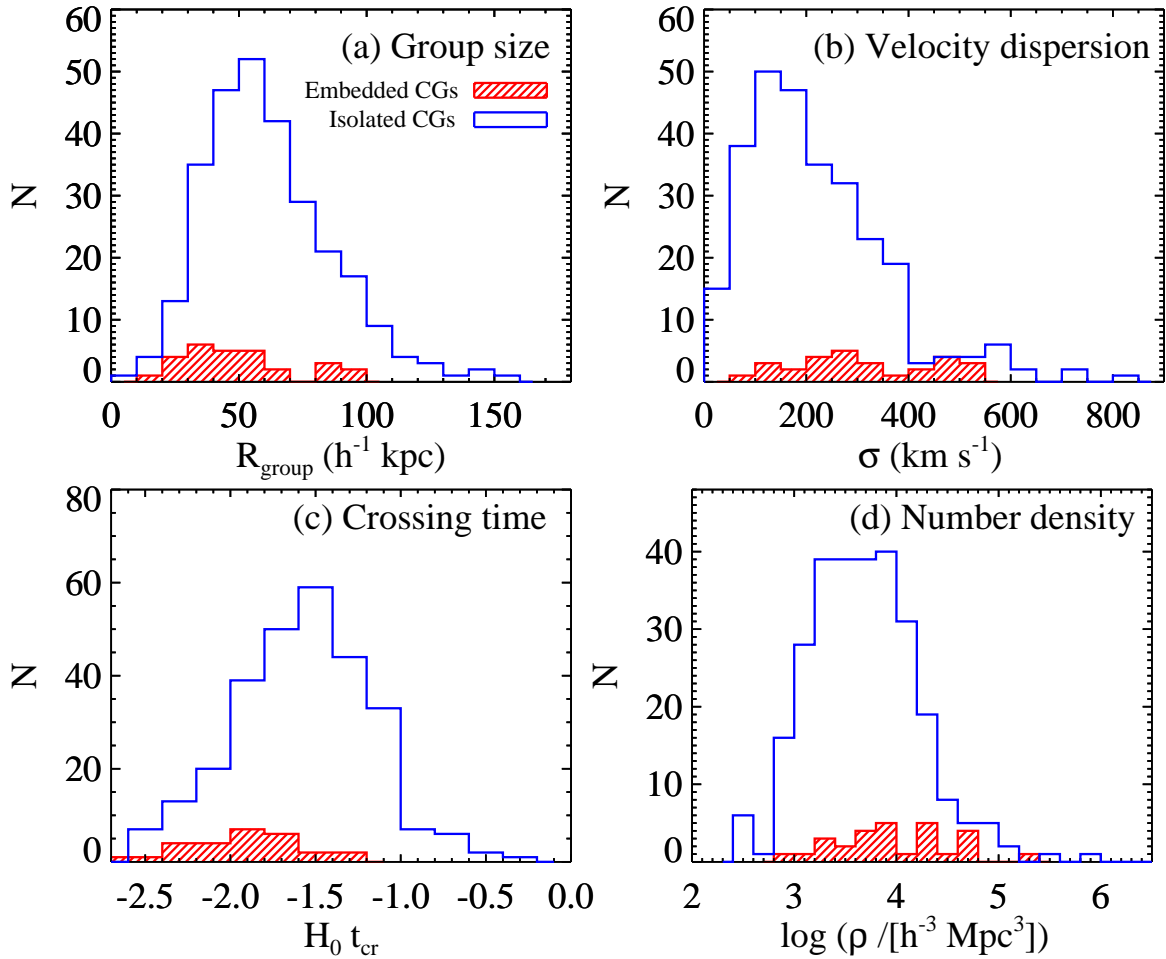


Figure 15. The physical properties of embedded (hatched histograms) and isolated (open histograms) compact groups including (a) group radius, (b) velocity dispersion, (c) crossing time, and (d) density. The embedded groups represent compact groups that have $\log(\Sigma_5)$ larger than 0.62.

the two groups are also significantly different (p-value from A-D test $\ll 0.01$). When we divide the compact groups into isolated and embedded systems based on the distance to nearby galaxy clusters, the difference in physical properties between the two types remains.

Compact groups based on Hickson’s selection criteria, including our original catalog of McConnachie et al. (2009), reflect a selection bias against dense local environments as a result of the isolation criterion. In other words, embedded compact groups may not fully represent the compact group population in high-density regions because many compact groups are missed in or near high-density regions as a result of the isolation criterion. The impact of this criterion is a function of the redshift of the group (Barton et al. 1996).

5. SUMMARY

By measuring new redshifts and incorporating redshifts from SDSS DR12 and other literature, we construct a catalog of 192 $N \geq 4$ compact groups with 799 member galaxies and 140 $N = 3$ complete compact groups with 420 member galaxies at $0.01 < z < 0.21$. In this

catalog, all member galaxies have spectroscopic redshifts. To date this catalog is the largest spectroscopically complete sample of these unusually dense systems. We explore the physical properties of the groups in this catalog and compare them with previous samples.

We examine the redshift dependence of physical properties of compact groups in the redshift range $0.01 < z < 0.21$. The velocity dispersion of compact groups changes little with redshift, indicating no significant evolution of dynamical masses of compact groups in this redshift range. The abundance of compact groups also shows no significant change with redshift. Thus it appears that either compact groups can survive longer than 1 Gyr or they continually reform by accreting new members from their surroundings.

The early-type fraction in our sample compact groups is 62%, slightly exceeding the fraction in the Hickson compact groups. We superimpose all of the compact groups in our sample to investigate the radial behavior of the velocity dispersion and morphological fraction. The velocity dispersion of early- and late-type galaxies are similar in $N \geq 4$ compact groups, but the dispersion

for the early-type galaxies is larger than for late-type galaxies in $N = 3$ compact groups. The velocity dispersions of early- and late-type galaxies in compact groups do not change much as a function of groupcentric radius. Compact groups enable examination of these issues at a galaxy density and spatial scale that are hard to access with any other systems.

We compare the catalog we construct with the Hickson and the DPOSS II samples that also have complete spectroscopy. We compare sizes, number densities, velocity dispersions and environments as measured by the fifth nearest neighbor to the group. The physical properties of our sample groups are similar to those for the Hickson compact groups, but they differ from those of the DPOSS II compact groups. The differences result from differences in the selection criteria for the DPOSS II and the Hickson compact groups. The parent catalog we use, McConnachie et al. (2009), is based on Hickson's criteria.

The local environments of compact groups are diverse. The Σ_5 distribution of compact groups is bimodal and 9% of compact groups are located in the denser region. This 'embedded' group fraction is lower than previous studies based on different local density tracers. The embedded compact groups are smaller and have larger velocity dispersion than the isolated compact groups on average.

Compact groups are a fascinating laboratory for studying galaxy evolution. Examination of the abundance of these systems over a larger redshift range and comparison with simulations may further constrain the formation and evolution of these systems. It is also important to clarify the subtle issues in the identification of the compact systems. Further exploration of identification directly from complete spectroscopic surveys in the nearby and moderate redshift universe would provide a further foundation for understanding the nature of these systems.

ACKNOWLEDGMENTS

We thank the anonymous referee for a very prompt report. We thank Perry Berlind and Michael Calkins, the remote observers at the Fred Lawrence Whipple Observatory, Jessica Mink, who processed the spectroscopic data, and all FAST queue observers who took data for this program. This paper uses data products produced by the OIR Telescope Data Center, supported by the Smithsonian Astrophysical Observatory. This work was supported by the National Research Foundation of Korea (NRF) grant funded by the Korea Government (MSIP) (No.2013R1A2A2A05005120). J.S. was supported by Global Ph.D. Fellowship Program through an NRF funded by the MEST (No. 2011-0007215). The research of M.J.G. is supported by the Smithsonian Institution. AD acknowledges partial support from the INFN grant InDark, the grant Progetti di Ateneo TO Call 2012 0011 'Marco Polo' of the University of Torino and the grant PRIN 2012 "Fisica Astroparticellare Teorica" of the Italian Ministry of University and Research. G.H.L. acknowledges the support

by the National Research Foundation of Korea (NRF) Grant funded by the Korean Government (NRF-2012-Fostering Core Leaders of the Future Basic Science Program).

REFERENCES

- Abazajian, K. N., Adelman-McCarthy, J. K., Agüeros, M. A., et al. 2009, The Seventh Data Release of the Sloan Digital Sky Survey, *ApJS*, 182, 543
- Adelman-McCarthy, J. K., Agüeros, M. A., Allam, S. S., et al. 2008, The Sixth Data Release of the Sloan Digital Sky Survey, *ApJS*, 175, 297
- Alam, S., Albareti, F. D., Allende Prieto, C., et al. 2015, The Eleventh and Twelfth Data Releases of the Sloan Digital Sky Survey: Final Data from SDSS-III, *ApJS*, 219, 12
- Andernach, H., & Coziol, R. 2005, The Relation of Compact Groups of Galaxies with Larger-Scale Structures, *ASPC*, 329, 67
- Athanassoula, E., Makino, J., Bosma, A. 1997, Evolution of Compact Groups of Galaxies - I. Merging Rates, *MNRAS*, 286, 825
- Barnes, J. 1985, The Dynamical State of Groups of Galaxies, *MNRAS*, 215, 517
- Barnes, J. E. 1989, Evolution of Compact Groups and the Formation of Elliptical Galaxies, *Nature*, 338, 123
- Barton, E., Geller, M., Ramella, M., Marzke, R. O., & da Costa, L. N. 1996, Compact Group Selection From Redshift Surveys, *AJ*, 112, 871
- Biviano, A., & Katgert, P. 2004, The ESO Nearby Abell Cluster Survey. XIII. The Orbits of the Different Types of Galaxies in Rich Clusters, *A&A*, 424, 779
- Bitsakis, T., Charmandaris, V., da Cunha, E., et al. 2011, A mid-IR Study of Hickson Compact Groups. II. Multiwavelength Analysis of the Complete GALEX-Spitzer Sample, *A&A*, 533, A142
- Bitsakis, T., Charmandaris, V., Appleton, P. N., et al. 2014, Herschel Observations of Hickson Compact Groups of Galaxies: Unveiling the Properties of Cold Dust, *A&A*, 565, A25
- Carlberg, R. G., Yee, H. K. C., & Ellingson, E. 1997, The Average Mass and Light Profiles of Galaxy Clusters, *ApJ*, 478, 462
- Choi, Y.-Y., Park, C., & Vogeley, M. S. 2007, Internal and Collective Properties of Galaxies in the Sloan Digital Sky Survey, *ApJ*, 658, 884
- Choi, Y.-Y., Han, D.-H., & Kim, S. S. 2010, Korea Institute for Advanced Study Value-Added Galaxy Catalog, *JKAS*, 43, 191
- Colless, M., & Dunn, A. M. 1996, Structure and Dynamics of the Coma Cluster, *ApJ*, 458, 435
- Coziol, R., Brinks, E., & Bravo-Alfaro, H. 2004, The Relation between Galaxy Activity and the Dynamics of Compact Groups of Galaxies, *AJ*, 128, 68
- da Costa, L. N., Geller, M. J., Pellegrini, P. S., et al. 1994, A Complete Southern Sky Redshift Survey, *ApJL*, 424, L1
- de Carvalho, R. R., Gonçalves, T. S., Iovino, A., et al. 2005, A Catalog of Distant Compact Groups Using the Digitized Second Palomar Observatory Sky Survey, *AJ*, 130, 425
- Danese, L., de Zotti, G., & di Tullio, G. 1980, On Velocity Dispersions of Galaxies in Rich Clusters, *A&A*, 82, 322
- Diaferio, A., Geller, M. J., & Ramella, M. 1994, The For-

- mation of Compact Groups of Galaxies. I: Optical Properties, *AJ*, 107, 868
- Diaferio, A., & Geller, M. J. 1996, Galaxy Pairwise Velocity Distributions on Nonlinear Scales, *ApJ*, 467, 19
- Díaz-Giménez, E., Mamon, G. A., Pacheco, M., Mendes de Oliveira, C., & Alonso, M. V. 2012, Compact Groups of Galaxies Selected by Stellar Mass: the 2MASS Compact Group Catalogue, *MNRAS*, 426, 296
- Díaz-Giménez, E., & Zandivarez, A. 2015, Where are Compact Groups in the Local Universe?, *A&A*, 578, A61
- Duplancic, F., O'Mill, A. L., Lambas, D. G., Sodr e, L., & Alonso, S. 2013, Galaxy triplets in Sloan Digital Sky Survey Data Release 7 - II. A connection with compact groups?, *MNRAS*, 433, 3547
- Einasto, M., Einasto, J., M uller, V., Hein am aki, P., & Tucker, D. L. 2003, Environmental Enhancement of Loose Groups around Rich Clusters of Galaxies, *A&A*, 401, 851
- Fabricant, D., Cheimets, P., Caldwell, N., & Geary, J. 1998, The FAST Spectrograph for the Tillinghast Telescope, *PASP*, 110, 79
- Fedotov, K., Gallagher, S. C., Durrell, P. R., et al. 2015, A Comprehensive HST BVI Catalogue of Star Clusters in Five Hickson Compact Groups of Galaxies, *MNRAS*, 449, 2937
- Geller, M. J., & Peebles, P. J. E. 1973, Statistical Application of the Virial Theorem to Nearby Groups of Galaxies, *ApJ*, 184, 329
- Geller, M. J., & Huchra, J. P. 1989, Mapping the Universe, *Science*, 246, 897
- Giovanelli, R., & Haynes, M. P. 1985, A 21 CM Survey of the Pisces-Perseus Supercluster. I - The Declination Zone +27.5 to +33.5 Degrees, *AJ*, 90, 2445
- Governato, F., Bhatia, R., & Chincarini, G. 1991, A Long-Lasting Compact Group, *ApJ*, 371, L15
- Hickson, P. 1982, Systematic Properties of Compact Groups of Galaxies, *ApJ*, 255, 382
- Hickson, P., Kindl, E., & Huchra, J. P. 1988, Morphology of Galaxies in Compact Groups, *ApJ*, 331, 64
- Hickson, P., Mendes de Oliveira, C., Huchra, J. P., & Palumbo, G. G. 1992, Dynamical Properties of Compact Groups of Galaxies, *ApJ*, 399, 353
- Hickson, P. 1997, Compact Groups of Galaxies, *ARAA*, 35, 357
- Hwang, H. S., & Lee, M. G. 2008, Galaxy Orbits for Galaxy Clusters in the Sloan Digital Sky Survey and Two Degree Field Galaxy Redshift Survey, *ApJ*, 676, 218
- Hwang, H. S., Elbaz, D., Lee, J. C., et al. 2010, Environmental Dependence of Local Luminous Infrared Galaxies, *A&A*, 522, A33
- Hwang, H. S., Park, C., Elbaz, D., & Choi, Y.-Y. 2012, Activity in Galactic Nuclei of Cluster and Field Galaxies in the Local Universe, *A&A*, 538, A15
- Iovino, A., de Carvalho, R. R., Gal, R. R., et al. 2003, A New Sample of Distant Compact Groups from the Digitized Second Palomar Observatory Sky Survey, *AJ*, 125, 1660
- Kroupa, P. 2015, Galaxies as Simple Dynamical Systems: observational Data Disfavor Dark Matter and Stochastic Star Formation, *Canadian Journal of Physics*, 93, 169
- Kurtz, M. J., & Mink, D. J. 1998, RVSAO 2.0: Digital Redshifts and Radial Velocities, *PASP*, 110, 934
- Lee, B. C., Allam, S. S., Tucker, D. L., et al. 2004, A Catalog of Compact Groups of Galaxies in the SDSS Commissioning Data, *AJ*, 127, 1811
- Lee, G.-H., Hwang, H. S., Lee, M. G., et al. 2015, Galaxy Evolution in the Mid-infrared Green Valley: A Case of the A2199 Supercluster, *ApJ*, 800, 80
- L opez-Cruz, O., A norve, C., Birkinshaw, M., et al. 2014, The Brightest Cluster Galaxy in A85: The Largest Core Known So Far, *ApJL*, 795, L31
- Mahdavi, A., Geller, M. J., B ohringer, H., Kurtz, M. J., & Ramella, M. 1999, The Dynamics of Poor Systems of Galaxies, *ApJ*, 518, 69
- Mamon, G. A. 1987, The Dynamics of Small Groups of Galaxies. I - Virialized Groups, *ApJ*, 321, 622
- McConnachie, A. W., Patton, D. R., Ellison, S. L., & Simard, L. 2009, Compact Groups in Theory and Practice - III. Compact Groups of Galaxies in the Sixth Data Release of the Sloan Digital Sky Survey, *MNRAS*, 395, 255
- Mendel, J. T., Ellison, S. L., Simard, L., Patton, D. R., & McConnachie, A. W. 2011, Compact Groups in Theory and Practice - IV. The Connection to Large-Scale Structure, *MNRAS*, 418, 1409
- Mendes de Oliveira, C., & Hickson, P. 1991, The Luminosity Function of Compact Groups of Galaxies, *ApJ*, 380, 30
- Mendes de Oliveira, C., & Hickson, P. 1994, Morphology of Galaxies in Compact Groups, *ApJ*, 427, 684
- Muratov, A. L., & Gnedin, O. Y. 2010, Modeling the Metallicity Distribution of Globular Clusters, *ApJ*, 718, 1266
- Newman, A. B., Treu, T., Ellis, R. S., & Sand, D. J. 2013, The Density Profiles of Massive, Relaxed Galaxy Clusters. II. Separating Luminous and Dark Matter in Cluster Cores, *ApJ*, 765, 25
- Park, C., & Choi, Y.-Y. 2005, Morphology Segregation of Galaxies in Color-Color Gradient Space, *ApJ*, 635, L29
- Park, C., & Hwang, H. S. 2009, Interactions of Galaxies in the Galaxy Cluster Environment, *ApJ*, 699, 1595
- Peebles, P. J. E. 1976, A Cosmic Virial Theorem, *Ap&SS*, 45, 3
- Pompei, E., & Iovino, A. 2012, The DPOSS II Distant Compact Group Survey: the EMMI-NTT Spectroscopic Sample, *A&A*, 539, A106
- Prandoni, I., Iovino, A., & MacGillivray, H. T. 1994, Automated Search for Compact Groups of Galaxies in the Southern Sky, *AJ*, 107, 1235
- Ramella, M., Diaferio, A., Geller, M. J., & Huchra, J. P. 1994, The Birthplace of Compact Groups of Galaxies, *AJ*, 107, 1623
- Ribeiro, A. L. B., de Carvalho, R. R., Capelato, H. V., & Zepf, S. E. 1998, Structural and Dynamical Analysis of the Hickson Compact Groups, *ApJ*, 497, 72
- Rines, K., & Diaferio, A. 2006, CIRS: Cluster Infall Regions in the Sloan Digital Sky Survey. I. Infall Patterns and Mass Profiles, *AJ*, 132, 1275
- Rines, K., Geller, M. J., Diaferio, A., & Kurtz, M. J. 2013, Measuring the Ultimate Halo Mass of Galaxy Clusters: Redshifts and Mass Profiles from the Hectospec Cluster Survey (HeCS), *ApJ*, 767, 15
- Rose, J. A. 1977, A Survey of Compact Groups of Galaxies, *ApJ*, 211, 311
- Rood, H. J., & Struble, M. F. 1994, Spatial Coincidence between a Number of Hickson Compact Groups and Loose Groups or Clusters, *PASP*, 106, 413
- Sohn, J., Hwang, H. S., Lee, M. G., Lee, G.-H., & Lee, J. C. 2013, Activity in Galactic Nuclei of Compact Group Galaxies in the Local Universe, *ApJ*, 771, 106
- Tago, E., Saar, E., Tempel, E., et al. 2010, Groups of galaxies in the SDSS Data Release 7. Flux- and Volume-Limited Samples, *A&A*, 514, A102

Tempel, E., Tamm, A., Gramann, M., et al. 2014, Flux- and Volume-Limited Groups/Clusters for the SDSS Galaxies: catalogues and mass estimation, *A&A*, 566, A1